CHALMERS | UNIVERSITY OF GOTHENBURG

PREPRINT 2009:35

Weak Coupling of a Reynolds Model and a Stokes Model for Hydrodynamic Lubrication

B. NILSSON
P. HANSBO

Department of Mathematical Sciences
Division of Mathematics
CHALMERS UNIVERSITY OF TECHNOLOGY
UNIVERSITY OF GOTHENBURG
Göteborg Sweden 2009

Preprint 2009:35

Weak Coupling of a Reynolds Model and a Stokes Model for Hydrodynamic Lubrication

B. Nilsson and P. Hansbo

Department of Mathematical Sciences
Division of Mathematics
Chalmers University of Technology and University of Gothenburg
SE-412 96 Göteborg, Sweden
Göteborg, September 2009

Preprint 2009:35
ISSN 1652-9715

Matematiska vetenskaper
Göteborg 2009

Weak coupling of a Reynolds model and a Stokes model for hydrodynamic lubrication

B. Nilsson[1,*] and P. Hansbo[2]

[1] *Center for Applied Mathematics and Physics, Halmstad University, SE–301 18 Halmstad, Sweden*
[2] *Department of Mathematical Sciences, Chalmers University of Techology and University of Gothenburg, SE–412 96 Göteborg, Sweden*

SUMMARY

The Reynolds model is a reduced Stokes model, valid for narrow lubrication regions. In order to be able to handle locally non-narrow regions such as pits or grooves, often displaying rapid geometrical variations, there is a need to be able to transit to the more accurate Stokes model. A fundamental problem is how to couple the two models in a numerical simulation, preferably allowing for different meshes in the different domains. In this paper, we present a weak coupling method for Reynolds and Stokes models for lubrication computations, including the possibility of cavitation in the different regions. The paper concludes with a numerical example.

KEY WORDS: Reynolds problem, Stokes problem, interface coupling, cavitation, variational inequality, finite element method

1. INTRODUCTION

In approximating thin fluid films typically appearing in lubrication, simplifying assumptions (discussed below) introduced by Reynolds in the 19:th century [6] are typically introduced in order to remove the dimension associated with the thickness of the film. In many situations, one or more of these assumptions must be dropped in order to make accurate predictions of the actual flow. If, however, the Reynolds assumptions hold in a substantial part of the domain of interest, there is a large computational gain in making a model coupling between the Reynolds model and a more accurate model such as Stokes or Navier–Stokes equations. An example of such a coupling scheme, between Stokes' and Reynolds equations, is given by Stay and Barocas [7], who formulate the Reynolds problem in terms solely of the pressure and apply stress balance and velocity continuity conditions on the interface. In this paper we take a more direct approach in that we pose both the Stokes and Reynolds equations on mixed form with unknowns for velocity and pressure. In the Reynolds case, the velocity variable then represents the flow rate, i.e., the integral of the physical velocity across the interface thickness. In posing

*Correspondence to: Bertil Nilsson, Center for Applied Mathematics and Physics, Halmstad University, SE–301 18 Halmstad, Sweden

this mixed formulation, we obtain a natural coupling method based on convex minimization with constraints: divergence zero constraints in both the Stokes and Reynolds domains, and continuity constraints between the mean velocities across the coupling interface.

2. REYNOLDS EQUATION

The first mathematical approach to tribology was undertaken by Leonard Euler with a geometrical resistance theory of "dry" friction - the *Interlocking Asperity Theory*. Euler's theory provides us with the two well known terms for static and dynamic friction. The static friction coefficient is provided by the tangent of the asperity angle, while the dynamic friction coefficient is reduced by the kinetic term. But the true workhorse for many of years is of course the Reynolds equation [6]. It has been used successfully to determine the pressure distribution in the fluid film for a wide range of applications from bearings, seals to sheet metal forming processes.

In the spirit of Figure 1, where a typical channel is furnished with the x-axis oriented as the relative surface velocity $\boldsymbol{U}$ and z-axis upwards, he made the following assumptions:

1. Body forces are neglected, i.e. there are no extra fields of forces acting on the fluid.
2. The pressure is constant through the thickness of the film.
3. The curvature of surfaces is large compared with film thickness. Surface velocities need not be considered as varying in direction.
4. There is no slip at the boundaries.
5. The lubricant is Newtonian, i.e. stress is proportional to rate of shear.
6. The flow is laminar.
7. Fluid inertia is neglected.
8. The viscosity is constant through the film thickness.

Under these assumptions, the flow equations can be deduced as follows. (We include these derivations in order to clarify the mixed model to be used in the sequel).

2.1. Continuity of flow of a column

Consider a thin column of fluid of height $H(x, y)$ and base dx, dy, Figure 2. Fluid flows from the left at a rate q_x per unit width so the volume flow rate is $q_x dy$ into the column. The rate of flow out per unit width is

$$q_x + \frac{\partial q_x}{\partial x} dx, \tag{1}$$

where $\frac{\partial q_x}{\partial x}$ is the rate of change of flow in the x-direction. The actual flow out is

$$\left(q_x + \frac{\partial q_x}{\partial x} dx \right) dy. \tag{2}$$

In the y-direction the same argument applies. The flow rate in is $q_y dx$ and out is

$$\left(q_y + \frac{\partial q_y}{\partial y} dy \right) dx. \tag{3}$$

The vertical flow is rather different. If the floor of the column moves upwards at a velocity w_0 and if the roof moves upward as well at a speed w_H the volume of the column changes at a rate $(w_H - w_0)dxdy$. Although the base and roof are moving, at the instant considered the height is H, though a fraction of time later it will of course have altered.

An alternative possibility is that the floor and/or roof are porous, and fluid is flowing in at a velocity w_0 or out of the column at a velocity w_H. The fluid velocity can be considered constant over the very small base area $dxdy$ hence the increase of volume is at a rate $w_0 dxdy$ and fluid leaves at a rate $w_H dxdy$.

For continuity of flow, the fluid being of constant density, the rate flowing in must equal the rate flowing out. These can all be added up. Flowing into the column

$$q_x dy + q_y dx + w_0 dxdy, \tag{4}$$

and flowing out

$$\left(q_x + \frac{\partial q_x}{\partial x}dx\right)dy + \left(q_y + \frac{\partial q_y}{\partial y}dy\right)dx + w_H dxdy. \tag{5}$$

These two are equal, equating them and canceling,

$$\frac{\partial q_x}{\partial x}dxdy + \frac{\partial q_y}{\partial y}dydx + (w_H - w_0)dxdy = 0. \tag{6}$$

Now $dxdy$ is arbitrary and non zero, hence can be canceled giving the continuity of flow of a column as

$$\frac{\partial q_x}{\partial x} + \frac{\partial q_y}{\partial y} + (w_H - w_0) = 0. \tag{7}$$

If the top and bottom surfaces are impermeable, $w_H - w_0$ is the rate of change of height of the column according to time and may be written $\frac{\partial H}{\partial t}$. Having obtained the continuity it is necessary to look at the force balance of an element of the fluid.

2.2. Equilibrium of an element

Take a small element of fluid of sides dx, dy and dz, Figure 3, and consider first the forces in the x-direction only. On the left of the element there is a pressure p on the face of area $dydz$ giving a force of $pdydz$ acting to the right. On the opposite face the pressure is

$$p + \frac{\partial p}{\partial x}dx, \tag{8}$$

and the corresponding force is

$$\left(p + \frac{\partial p}{\partial x}dx\right)dydz. \tag{9}$$

There are shear stresses on the top and bottom faces producing forces. On the bottom face the shear stress τ_x gives a force $\tau_x dxdy$ acting to the left and on the top face, and acting to the right, is a force

$$\left(\tau_x + \frac{\partial \tau_x}{\partial z}dz\right)dxdy, \tag{10}$$

where the shear stress on the top face being $\tau_x + \frac{\partial \tau_x}{\partial z}dz$. These forces acting to the left and right must balance each other so

$$pdydz + \left(\tau_x + \frac{\partial \tau_x}{\partial z}dz\right)dxdy = \left(p + \frac{\partial p}{\partial x}dx\right)dydz + \tau_x dxdy, \tag{11}$$

expanding and canceling considering $dxdydz$ an arbitrary non zero volume gives

$$\frac{\partial \tau_x}{\partial z} = \frac{\partial p}{\partial x}. \tag{12}$$

Now Newton's viscosity relation states

$$\tau_x = \mu \frac{\partial u}{\partial z}, \tag{13}$$

where u is the velocity of the fluid in the x-direction, so

$$\frac{\partial}{\partial z}\left(\mu \frac{\partial u}{\partial z}\right) = \frac{\partial p}{\partial x}. \tag{14}$$

In the y-direction where the velocity of the fluid is v the shear stresses and pressures can be equated and a similar equation follows

$$\frac{\partial \tau_y}{\partial z} = \frac{\partial p}{\partial y}, \quad \text{where} \quad \tau_y = \mu \frac{\partial v}{\partial z},$$

so

$$\frac{\partial}{\partial z}\left(\mu \frac{\partial v}{\partial z}\right) = \frac{\partial p}{\partial y}. \tag{15}$$

The pressure gradient in the z-direction is by assumption zero, so $\frac{\partial p}{\partial z} = 0$. Consider now equation (14) further. This can be integrated since p is not a function of z, thus

$$\mu \frac{\partial u}{\partial z} = \frac{\partial p}{\partial x} z + C_1. \tag{16}$$

Now both μ and u are functions of z but it is in this context too difficult to consider both at once so μ is taken as constant with respect to z as stated in assumption 8. It is important to realize that this is a big assumption and is only made for simplicity. The inclusion of $\frac{\partial \mu}{\partial z}$ can modify the equation very considerably in certain circumstances. However, using this assumption, a further integration can be performed to give

$$\mu u = \frac{\partial p}{\partial x} \frac{z^2}{2} + C_1 z + C_2. \tag{17}$$

The boundary conditions are simple, according to assumption 4, i.e. no slip at the boundaries

$$\begin{cases} u(0) = U_0 \\ u(H) = U_H \end{cases}, \tag{18}$$

so (17) and (18) gives

$$u = \frac{1}{2\mu} \frac{\partial p}{\partial x}(z^2 - zH) + (U_H - U_0)\frac{z}{H} + U_0. \tag{19}$$

Finally the flow rate $q_x = \int_0^H u \, dz$ in the x-direction per unit width of y

$$q_x = -\frac{H^3}{12\mu} \frac{\partial p}{\partial x} + (U_0 + U_H)\frac{H}{2}. \tag{20}$$

If the same procedure is followed for y using equation (15) it is easily found that

$$q_y = -\frac{H^3}{12\mu}\frac{\partial p}{\partial y} + (V_0 + V_H)\frac{H}{2}, \tag{21}$$

where V_0 and V_H in the y-direction correspond to U_0 and U_H in the x-direction.

It is now possible to replace (20) and (21) into the continuity equation (7)

$$\begin{aligned}\frac{\partial}{\partial x}\left(\frac{H^3}{\mu}\frac{\partial p}{\partial x}\right) + \frac{\partial}{\partial y}\left(\frac{H^3}{\mu}\frac{\partial p}{\partial y}\right) = 6\Big(\frac{\partial}{\partial x}\left((U_0 + U_H)\,H\right) + \\ \frac{\partial}{\partial y}\left((V_0 + V_H)\,H\right) + 2\,(w_H - w_0)\Big).\end{aligned} \tag{22}$$

This is the full Reynolds equation in terms of the pressure as usually stated, and in particular as used in [7].

3. A MIXED FORMULATION OF THE REYNOLDS EQUATION

In order to formulate a coupling method between Reynolds equation and more accurate fluid models, we reintroduce the flow rates from (20)–(21) and pose the problem as that of finding $(\boldsymbol{q}, p)$ such that

$$\begin{aligned}\frac{12\mu}{H^3}\boldsymbol{q} + \nabla p &= \frac{6\mu}{H^2}\boldsymbol{U},\\ \nabla\cdot\boldsymbol{q} &= 0.\end{aligned}$$

where it has been assumed that the thickness of the film does not change over time and that $\boldsymbol{U} = (U_0, U_H) = (0, U_H)$ and $\boldsymbol{V} = \boldsymbol{0}$. We note in particular that from the way we have derived this equation, $\boldsymbol{q}$ denotes the integral of velocity over height (rather than the mean velocity).

In weak form, this problem may be written as seeking $\boldsymbol{q} \in H(\mathrm{div};\Omega)$, where

$$H(\mathrm{div};\Omega) = \{\boldsymbol{v} \in [L_2(\Omega)]^2 : \|\nabla\cdot\boldsymbol{v}\|_{L_2(\Omega)} < \infty\},$$

and $p \in L_2(\Omega)$, $L_2(\Omega)$ being the space of square–integrable functions over Ω, such that

$$\int_\Omega \frac{12\mu}{H^3}\boldsymbol{q}\cdot\boldsymbol{v}\,d\Omega - \int_\Omega p\,\nabla\cdot\boldsymbol{v}\,d\Omega = \int_\Omega \frac{6\mu}{H^2}\boldsymbol{U}\cdot\boldsymbol{v}\,d\Omega, \quad \forall\boldsymbol{v}\in H(\mathrm{div};\Omega), \tag{23}$$

and

$$\int_\Omega \nabla\cdot\boldsymbol{q}\,w\,d\Omega = 0, \quad \forall w \in L_2(\Omega). \tag{24}$$

Boundary conditions for this problem are either handled strongly, in the case of conditions on the normal flow rate, or weakly in the case of conditions on the pressure.

4. THE COUPLED PROBLEM

We are interested in coupling the Reynolds model with the Stokes model across a vertical interface. The interface from the Reynolds side then appears one–dimensional, while the

interface on the Stokes side is two–dimensional. Denote by Ω_R the Reynolds domain, Ω_S the Stokes domain, by $\Gamma_{1\mathrm{D}}$ the dimensionally reduced interface, and by $\Gamma_{2\mathrm{D}} := \Gamma_{1\mathrm{D}} \times H$ the full 2D interface. We have the following problem to solve, not taking cavitation into consideration:

$$\begin{aligned} \frac{12\mu}{H^3}\boldsymbol{q} + \nabla p_R &= \frac{6\mu}{H^2}\boldsymbol{U} \text{ in } \Omega_R \subset \mathbb{R}^2, \\ \nabla \cdot \boldsymbol{q} &= 0 \text{ in } \Omega_R, \\ -\mu\Delta\boldsymbol{u} + \nabla p_S &= 0 \text{ in } \Omega_S \subset \mathbb{R}^3, \\ \nabla \cdot \boldsymbol{u} &= 0 \text{ in } \Omega_S, \\ \int_0^H \sigma_n(\boldsymbol{u}, p_S)\, dz + p_R &= 0 \text{ on } \Gamma_{1\mathrm{D}}, \\ (\boldsymbol{q} - \int_0^H \boldsymbol{u}\, dz) \cdot \boldsymbol{n} &= 0 \text{ on } \Gamma_{1\mathrm{D}}. \end{aligned} \tag{25}$$

This problem must then be supplemented with boundary conditions on the exterior boundaries, which depend on the type of model adjacent to the exterior. These are handled in the usual way in the finite element setting.

We also wish to be able to include cavitation into our numerical model. Cavitation occurs when the pressure reaches atmospheric pressure, which we for definiteness define as $p = 0$. The lubricant cannot support subatmospheric pressure, so an additional condition is $p \geq 0$ in $\Omega_R \cup \Omega_S$. In order to incorporate this condition into the model, it can be written as a variational inequality (cf. Section 4.1). For this purpose we introduce the space of admissible pressures

$$K = \{p \in L_2(\Omega) : p \geq 0\},$$

which is a convex subspace of $L_2(\Omega)$.

4.1. Finite element formulation

To formulate our discrete method, we suppose that we have regular finite element partitions $\mathcal{T}_h^i$, $i \in \{R, S\}$ of the two subdomains Ω_R and Ω_S into shape regular simplexes. These two meshes imply the existence of trace meshes on the interface

$$\mathcal{G}_h^i = \{E : E = T \cap \Gamma_{2\mathrm{D}}, \forall T \in \mathcal{T}_h^i\},\ i \in \{R, S\}.$$

From the finite element theory of mixed methods, it is well known that one must carefully select the combination of approximations for the flow variables and the pressure. In the case of the Reynolds model, a well known stable element combination is the lowest order Raviart-Thomas approximation for the flow rate, i.e., $\boldsymbol{q}^h \in V_h^R$, where

$$V_h^R := \{\boldsymbol{q} \in H(\mathrm{div}; \Omega) : \boldsymbol{q}|_T \in (P_0(T))^2 + \boldsymbol{x}P_0(T), \forall T \in \mathcal{T}_h^R\}$$

combined with a pressure space of elementwise constant pressures,

$$Q_h^R := \{p \in L_2(\Omega) : p|_T \in P_0(T), \forall T \in \mathcal{T}_h^R\}.$$

In the case of Stokes flow, we choose to use the well known stable Taylor-Hood element consisting of the velocity space

$$V_h^S := \{\boldsymbol{u} \in [C^0(\Omega)]^3 : \boldsymbol{u}|_T \in (P_2(T))^3, \forall T \in \mathcal{T}_h^S\}$$

and pressure space

$$Q_h^S := \{p \in C^0(\Omega) : p|_T \in P_1(T),\, \forall T \in \mathcal{T}_h^S\}.$$

We shall use a Lagrange multiplier method using piecewise constants on the 1D trace mesh $\mathcal{G}_h^R$ for the fulfillment of the continuity requirement on the velocities. We seek $(\boldsymbol{q}^h, \boldsymbol{u}^h, p_R^h, p_S^h, \lambda^h) \in V_h^R \times V_h^S \times Q_h^R \times Q_h^S \times \mathcal{C}_h$, where

$$\mathcal{C}_h := \{\kappa \in L_2(\Gamma_{1\mathrm{D}}) : \kappa|_E \in P_0(E),\, \forall E \in \mathcal{G}_h^R\},$$

such that

$$\begin{aligned} a_h((\boldsymbol{q}^h, \boldsymbol{u}^h), (\boldsymbol{v}_R, \boldsymbol{v}_S)) + b_h((p_R^h, p_S^h), (\boldsymbol{v}_R, \boldsymbol{v}_S)) + c_h(\lambda^h, (\boldsymbol{v}_R, \boldsymbol{v}_S)) = f_h(\boldsymbol{v}_R), \\ \forall (\boldsymbol{v}_R, \boldsymbol{v}_S) \in V_h^R \times V_h^S, \end{aligned} \tag{26}$$

$$b_h((p_R^h - w_R, p_S^h - w_S), (\boldsymbol{q}^h, \boldsymbol{u}^h)) \le 0, \quad \forall (w_R, w_S) \in (Q_h^R \cap K) \times (Q_h^S \cap K), \tag{27}$$

and

$$c_h(\kappa, (\boldsymbol{q}^h, \boldsymbol{u}^h)) = 0, \quad \forall \kappa \in \mathcal{C}_h. \tag{28}$$

Here

$$\begin{aligned} a_h((\boldsymbol{q}, \boldsymbol{u}), (\boldsymbol{v}_R, \boldsymbol{v}_S)) &:= \int_{\Omega_R} \frac{12\mu}{H^3} \boldsymbol{q} \cdot \boldsymbol{v}_R \, d\Omega + \int_{\Omega_S} \mu \nabla \boldsymbol{u} : \nabla \boldsymbol{v}_S \, d\Omega, \\ b_h((w_R, w_S), (\boldsymbol{v}_R, \boldsymbol{v}_S)) &:= -\int_{\Omega_R} w_R \nabla \cdot \boldsymbol{v}_R \, d\Omega - \int_{\Omega_S} w_S \nabla \cdot \boldsymbol{v}_S \, d\Omega, \\ c_h(\gamma, (\boldsymbol{v}_R, \boldsymbol{v}_S)) &:= \int_{\Gamma_{2\mathrm{D}}} \gamma \, \boldsymbol{n} \cdot (\boldsymbol{v}_R - \int_0^H \boldsymbol{v}_S \, dz) \, ds, \\ f_h(\boldsymbol{v}_R) &:= \int_{\Omega_R} \frac{6\mu}{H^2} \boldsymbol{U} \cdot \boldsymbol{v}_R \, d\Omega. \end{aligned} \tag{29}$$

It is clear from the formulation that on every one–dimensional element side on $\mathcal{G}_h^R$ the (constant) normal component of the flow rate will be set equal to the mean of the Stokes velocities over the height (multiplied by the height). The problem could thus alternatively be posed in a discrete space where this side condition is used directly in the definition of the space. The the well–posedness of the variational inequality (26–27), without the coupling condition, follows from the general theory presented by Brezzi, Hager, and Raviart [2] (cf. [4, 5] for further details); for the the stability of the coupling condition in particular, we refer to the closely related approach of Alonso et al. [1] (dealing with 2D–2D coupling).

4.2. Solution

For solving the nonlinear saddle point problem resulting from the finite element discretization, we have chosen to use an Uzawa iteration method. In order to find a good initial solution, we first assemble the finite element matrices emanating from the full model, written using the unrestricted spaces (that are actually used in the iterations)

$$\begin{pmatrix} \mathbf{K}_S & \mathbf{B}_d & \mathbf{0} & \mathbf{0} & \mathbf{C}_S \\ \mathbf{B}_d^T & \mathbf{0} & \mathbf{0} & \mathbf{0} & \mathbf{0} \\ \mathbf{0} & \mathbf{0} & \mathbf{K}_q & \mathbf{K}_p & \mathbf{C}_R \\ \mathbf{0} & \mathbf{0} & \mathbf{K}_p^T & \mathbf{0} & \mathbf{0} \\ \mathbf{C}_S^T & \mathbf{0} & \mathbf{C}_R^T & \mathbf{0} & \mathbf{0} \end{pmatrix} \begin{pmatrix} \mathbf{u}^h \\ \mathbf{p}_S^h \\ \mathbf{q}^h \\ \mathbf{p}_R^h \\ \boldsymbol{\lambda}^h \end{pmatrix} = \begin{pmatrix} \mathbf{0} \\ \mathbf{0} \\ \mathbf{F}_q \\ \mathbf{0} \\ \mathbf{0} \end{pmatrix}, \tag{30}$$

where the submatrices are the assembled element matrices according to the integrals found in (29), i.e. with $(\boldsymbol{v}_R, \boldsymbol{v}_S, w_R, w_S, \kappa) \in V_h^R \times V_h^S \times Q_h^R \times Q_h^S \times \mathcal{C}_h$ denoting generic basis functions spanning the relevant spaces, we have

$$\mathbf{K}_S = \bigoplus_{T\in\mathcal{T}_h^S} \int_T \mu \nabla \boldsymbol{v}_S : \nabla \boldsymbol{v}_S \, d\Omega, \; \mathbf{B}_d = -\bigoplus_{T\in\mathcal{T}_h^S} \int_T w_S \nabla\cdot \boldsymbol{v}_S \, d\Omega,$$

$$\mathbf{K}_q = \bigoplus_{T\in\mathcal{T}_h^R} \int_T \frac{12\mu}{H^3} \boldsymbol{v}_R \cdot \boldsymbol{v}_R \, d\Omega, \; \mathbf{K}_p = \bigoplus_{T\in\mathcal{T}_h^R} \int_T w_R \nabla\cdot \boldsymbol{v}_R \, d\Omega,$$

$$\mathbf{F}_q = \bigoplus_{T\in\mathcal{T}_h^R} \int_T \frac{6\mu}{H^2} \boldsymbol{U} \cdot \boldsymbol{v}_R \, d\Omega,$$

$$\mathbf{C}_R = \bigoplus_{E\in\mathcal{G}_h^R} \int_E \boldsymbol{n} \cdot \boldsymbol{v}_R \, ds, \; \mathbf{C}_S = -\bigoplus_{E\in\mathcal{G}_h^R} \int_E \int_0^H \boldsymbol{n} \cdot \boldsymbol{v}_S \, dz \, ds, ,$$

where $\oplus$ denotes the assembly operator for the finite element matrix construction. The system (30) is fed repeatedly into a direct linear equation solver. In each round is a simple cavitation requirement $p_S^h = \max(p_S^h, 0)$ enforced and a modification of the corresponding residuals (out–of–balance residual forces) carried out. This process is repeated until $p_S^h \geq 0$ throughout the domain. The artificial pressure boundary conditions are then released and the model with current solution state is handed over to Usawa taking cavitation into consideration using a pressure projection on the run. The Stokes and Reynolds models are solved in parallel as follows.

A core operation in Uzawa algorithm is to update the pressure field. However, recall that $p = -\lim_{\kappa\to\infty} \kappa \nabla\cdot \boldsymbol{u}$, but $\nabla\cdot V_h^S$ does not reside in Q_h^S, due to the fact that we are using Taylor-Hood elements, so in step 3 we find a continuous pressure corrector $p_d \in Q_h^S$.

1. Let $k = 0$ and choose as initial pressure solution ${}^k\mathbf{p}_S^h$ and ${}^k\mathbf{p}_R^h$ provided by the solution strategy of the linear system (30) just described.
2. Solve the condensated version of the linear system (30)
$$\begin{pmatrix} \mathbf{K}_S & \mathbf{0} & \mathbf{C}_S \\ \mathbf{0} & \mathbf{K}_q & \mathbf{C}_R \\ \mathbf{C}_S^T & \mathbf{C}_R^T & \mathbf{0} \end{pmatrix} \begin{pmatrix} {}^k\mathbf{u}^h \\ {}^k\mathbf{q}^h \\ {}^k\boldsymbol{\lambda}^h \end{pmatrix} = \begin{pmatrix} -\mathbf{B}_d {}^k\mathbf{p}_S^h \\ \mathbf{F}_q - \mathbf{K}_p {}^k\mathbf{p}_R^h \\ \mathbf{0} \end{pmatrix},$$
for the vector fields ${}^k\mathbf{u}^h$ and ${}^k\mathbf{q}^h$ and the Lagrange multipliers ${}^k\boldsymbol{\lambda}^h$.
3. Find a continuous pressure corrector $p_d \in Q_h^S$ from the system
$$\textstyle\int_{\Omega_S} p_d q \, d\Omega = -\int_{\Omega_S} \nabla\cdot \boldsymbol{u}^h q \, d\Omega, \; \forall q \in Q_h^S \;\Leftrightarrow\; \mathbf{M}_d \mathbf{p}_d = \mathbf{B}_d {}^k\mathbf{u}^h,$$
where $\mathbf{M}_d$ is the lumped mass matrix, which makes the update fast.
4. Update pressure fields
$$\begin{cases} {}^{k+1}\mathbf{p}_S^h = P_\Lambda({}^k\mathbf{p}_S^h + \omega_S \mathbf{p}_d) \\ {}^{k+1}\mathbf{p}_R^h = P_\Lambda(\mathbf{F}_q + \omega_R \mathbf{K}_p^T {}^k\mathbf{q}^h) \end{cases}$$
where ω_S and ω_R are relaxation parameters and the operator $P_\Lambda(\boldsymbol{\vartheta}) := \max(\mathbf{0}, \boldsymbol{\vartheta})$.
5. If convergence not yet achieved, set $k = k + 1$ and go back to step 2.

The projection operator P_Λ is applied point–wise on the nodal values for the pressure in

the Stokes case and element–wise in the Reynolds case, which by construction leads to $\{p_R^h, p_S^h\} \in K$.

The typical number of iterations is then 200 for the Usawa algorithm, using well tuned relaxation for the two models, to converge according to $\|^{k+1}\mathbf{p}_S^h - {}^k\mathbf{p}_S^h\| + \|^{k+1}\mathbf{p}_R^h - {}^k\mathbf{p}_R^h\| < 10^{-9}$ for a particular mesh. For the numerical evaluation of the integrals involved in the coupling matrices, $\mathbf{C}_R$ and $\mathbf{C}_S$, a 2-point Gauss quadrature scheme is used on the edges of the one-dimensional trace mesh $\mathcal{G}_h^R$ and a 3-point Gauss quadrature scheme for companion surface integrals on the Stokes mesh.

5. NUMERICAL EXAMPLE

In order to investigate the performance of the method proposed, a numerical example will be presented. Of course, experimental results demonstrating in detail the local behavior of the pressure and velocity images for the two physical models glued together is hard to achieve.

The object for our study is a single parabolic shaped oil pocket, Figure 4. A central longitudinal cut through the gap between the sheet metal and work piece comprise our full symmetrical 3D computational Stokes model. The nominal channel has the dimensions $x \times y \times z = [-0.5, 0.5] \times [0, 0.6] \times [0, 0.2]$ and the particular parabolic oil pocket is shaped as $(x/0.4)^2 + (y/0.4)^2 + (z/0.1)^2 = 1$. The narrow lubrication regions modeled by Reynolds equation is used as transit parts between the Stokes models. We investigate one Stokes part combined with two Reynolds parts of rectangular shape, the inlet part $x \times y = [-1.6, -0.5] \times [0, 0.6]$ and the outlet part $x \times y = [0.5, 1.6] \times [0, 0.6]$. The finite element model can be inspected in Figure 5.

Boundary conditions used for the pressure is $p = 0$ at inlet $x = -1.6$ and outlet $x = 1.6$ parts of the narrow Reynolds regions. Velocity is set to $u_x = u_y = u_z = 0$ over the floor of the Stokes channel, oil pocket included. Symmetry along the two cuts $y = 0$ and $y = 0.6$ is accomplished via $u_y = 0$ for the Stokes part and $q = 0$ for the Reynolds parts. Finally, the flow is driven by $u_x = 1, u_y = u_z = 0$ at the ceiling of the Stokes model and over the Reynolds parts. The lubricant viscosity $\mu = 1$.

For visualization purposes we apply a L_2-projection of the Reynolds constant element pressure field forming a continuous one. In Figure 6 we present pressure contour lines on the model surface, and in Figures 7 and 8 contour lines for slices in two different directions. We can clearly identify by inspection the cavitation zone upstream in the pocket and a high pressure peak at downstream pocket side. An important point is that we do not need to *a priori* define the boundary location between the fluid and cavitation phases. The classical way to approach the cavitation problem in the Reynolds community via continuity boundary conditions or first computing p_R from a pure Reynolds solution, followed by approximating $p \approx \max(0, p_R)$ (known as the half-Sommerfeld condition), is not very accurate compared to the cavitation model presented here.

From Figure 9 it is obvious that the weak coupling of velocity field between the models produce a Couette flow profile as expected.

If we define pocket impact to be the ratio of maximal channel height over minimal channel height Figure 10 indicates that the model at hand yields better lift for oil pocket impacts of $\gtrapprox 1.9$ compared to simpler models (included in the figure purely for qualitative comparison). This is in agreement with our earlier observation described in Hansbo and Nilsson [3, 4]. Note

that as the oil pocket depth increases, recirculation appears in the pocket; this violates one of the basic assumptions in Reynolds model. No such limitation afflicts Stokes flow, which is the strongest argument for employing this more complex model.

REFERENCES

1. Alonso A, Dello Russo A, Padra C, Rodríguez R. An adaptive finite element scheme to solve fluid–structure vibration problems on non-matching grids *Computing and Visualization in Science* 2001; **4**:67–78
2. Brezzi F, Hager WW, Raviart PA Error estimates for the finite element solution of variational inequalities. Part II. Mixed methods, *Numerische Mathematik* 1978; **31**:1–16.
3. Nilsson B., Hansbo P. Adaptive finite element methods for hydrodynamic lubrication with cavitation, *International Journal for Numerical Methods in Engineering* 2007; **72**:1584–1604.
4. Nilsson B, Hansbo P. A Stokes model with cavitation for the numerical simulation of hydrodynamic lubrication, Preprint, Department of Mathematical Sciences, Chalmers University of Technology, 2008.
5. Nilsson B. A mixed finite element formulation of Reynolds equations with cavitation, Preprint, Department of Mathematical Sciences, Chalmers University of Technology, 2009.
6. Reynolds O. On the theory of lubrication and its application to Beauchamp Tower's experiments, including an experimental determination of the viscosity of olive oil. *Philosophical Transactions of the Royal Society of London, Series A* 1886; **177**:157–233.
7. Stay MS, Barocas VH Coupled lubrication and Stokes flow finite elements, *International Journal for Numerical Methods Fluids* 2003; **43**:129–146.

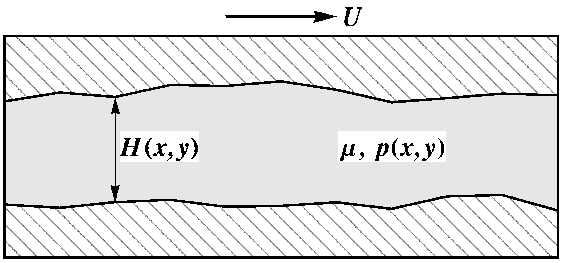

Figure 1. Reynolds channel.

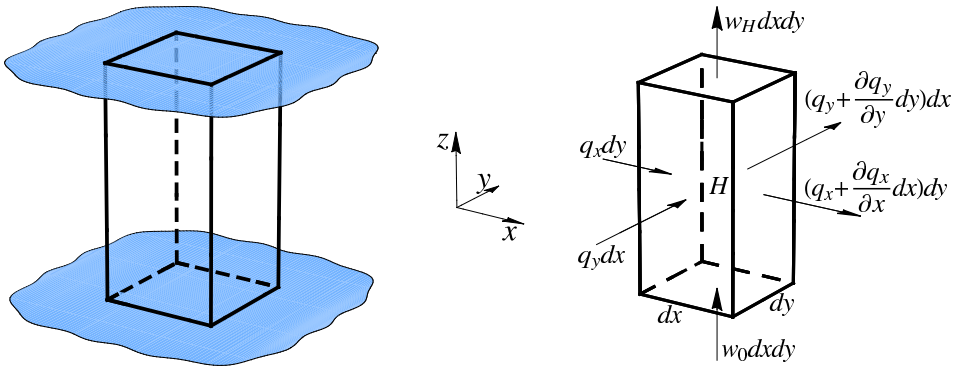

Figure 2. Continuity of flow in a column of height H.

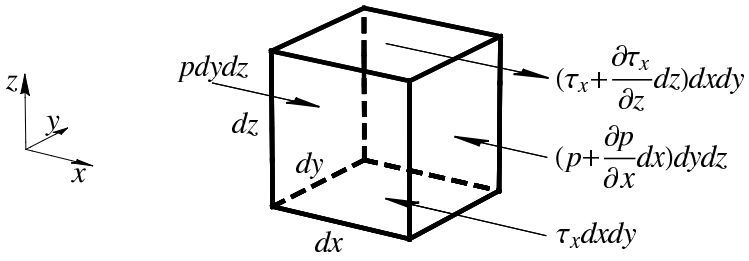

Figure 3. Equilibrium of an element.

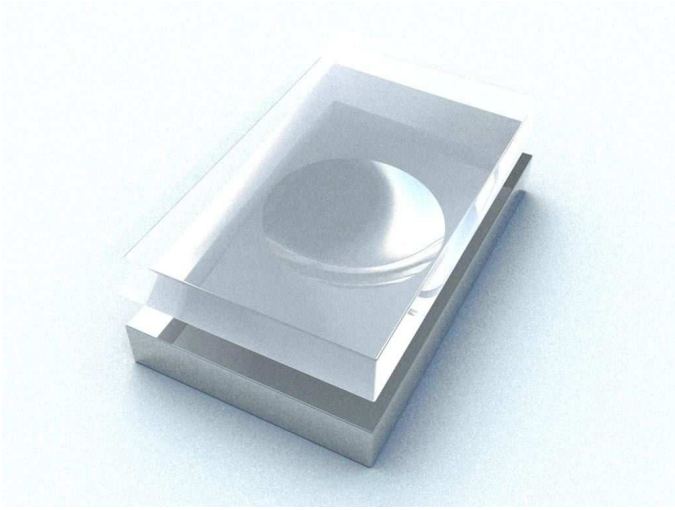

Figure 4. Oil pocket model.

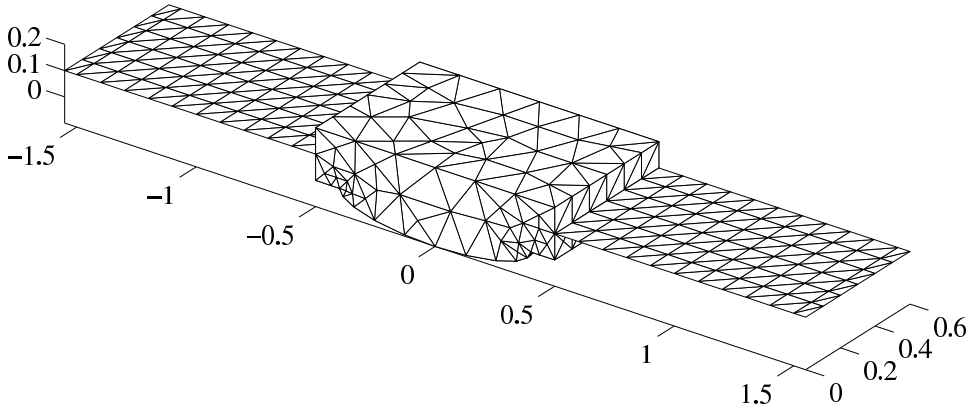

(a) FE-model from above.

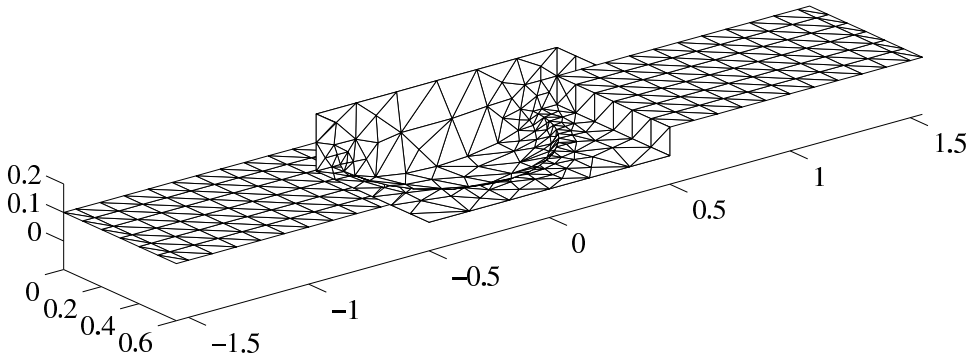

(b) FE-model from below.

Figure 5. Finite element computational model. Outlet and inlet 2D Reynolds parts and 3D Stokes part in between.

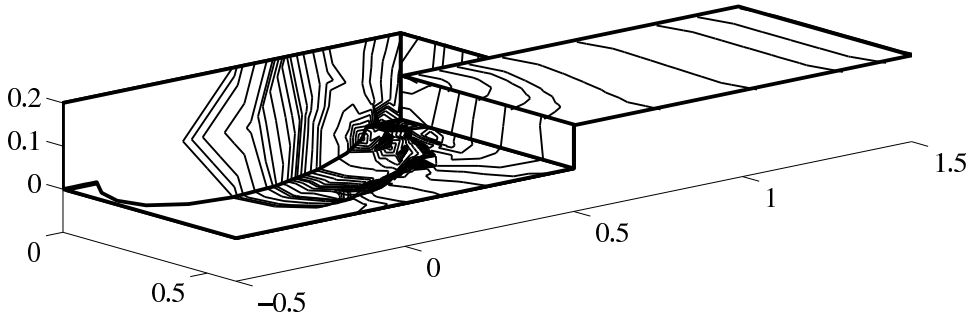

Figure 6. Pressure contour lines on the surface.

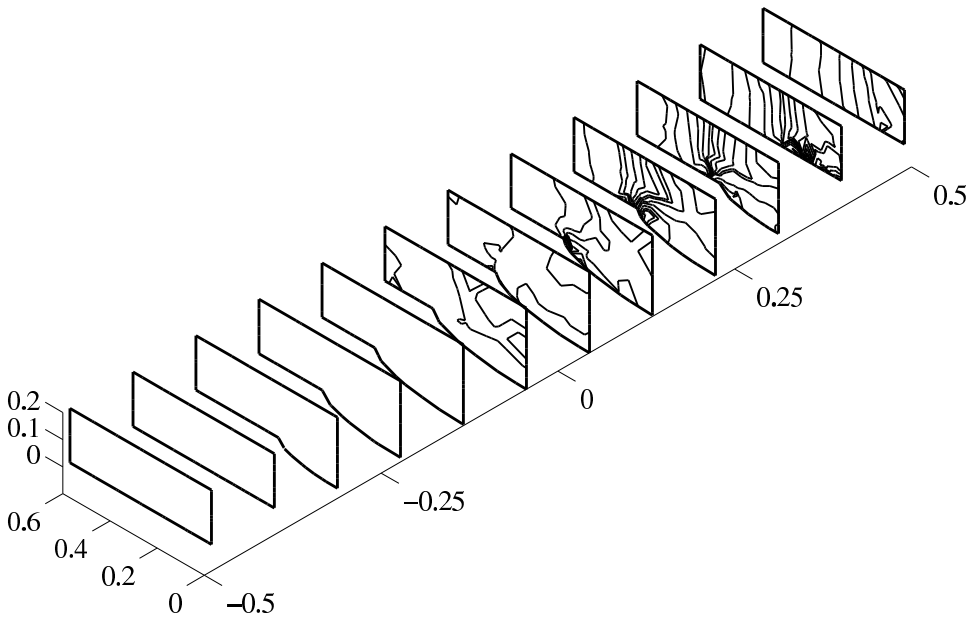

Figure 7. Pressure contour lines on x-slices.

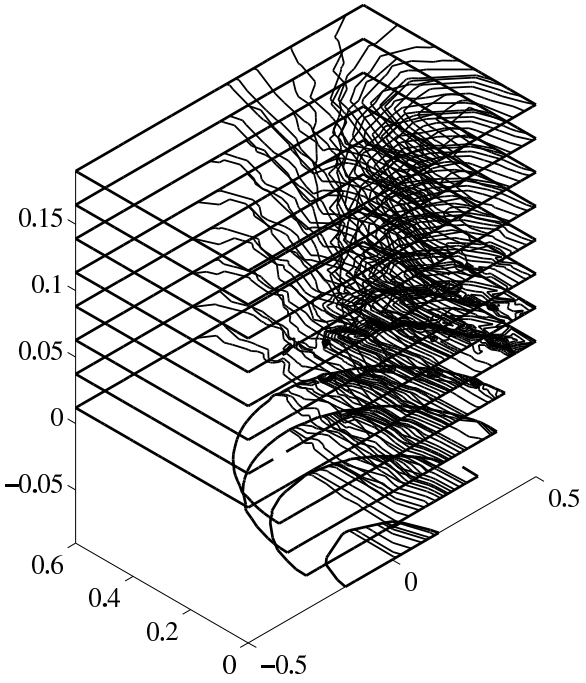

Figure 8. Pressure contour lines on z-slices.

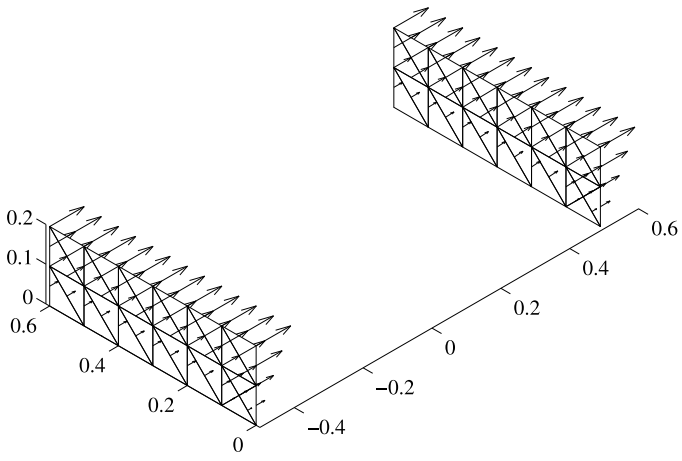

Figure 9. Couette flow profile at coupling zones.

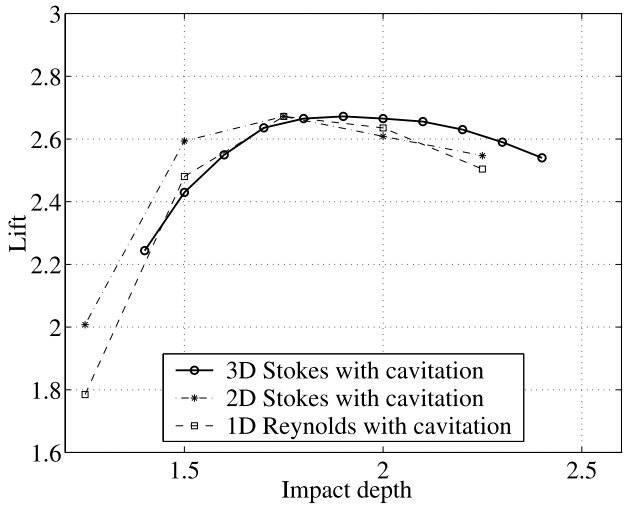

Figure 10. Lift for present coupling model. Normalized lift is included for the 2D Stokes and 1D Reynolds models just for qualitative comparison.